Available online at www.sciencedirect.com
ScienceDirect
Carbohydrate Research 342 (2007) 2776–2792
Carbohydrate RESEARCH

Characterization of the chemical degradation of hyaluronic acid during chemical gelation in the presence of different cross-linker agents

Atoosa Maleki, Anna-Lena Kjøniksen* and Bo Nyström

Department of Chemistry, University of Oslo, PO Box 1033, Blindern, N-0315 Oslo, Norway

Received 31 May 2007; received in revised form 27 August 2007; accepted 29 August 2007
Available online 6 September 2007

Abstract—Dynamic light scattering (DLS) and rheological experiments have been performed on semidilute aqueous hyaluronic acid (HA) solutions during the chemical cross-linking process with a water-soluble carbodiimide (WSC) to produce a hydrogel. The formation and destruction of the gel are characterized. The results suggest that the gel is cross-linked via ester linkages and at later stage in the process, the omnipresent hydrolysis of interpolymer ester linkages and glycosidic bonds prevails, leading to disruption of the gel. The process of forming and breaking the gel is affected by the cross-linker concentration and pH. The cross-linking of HA with WSC in the presence of L-lysine methyl ester produced a gel with a longer time of gelation and the degradation of the gel was prolonged because of the more stable amide bond formation as the cross-link. By using the Ugi multicomponent condensation reaction, interpolymer cross-linking occurs via the formation of amide linkages and a stable gel evolves, which is only slightly degraded over an extended time window. DLS measurements on HA solutions with WSC show the emergence of a long-time power-law tail in the correlation functions at conditions both before and beyond the viscosity maximum. At a late stage in the gel-breakage regime, the power-law profile of the decay disappears and the long-time tail of the correlation function can be portrayed by a stretched exponential. The findings indicate that the power-law feature is associated with the confinement of chain dynamics and anomalous diffusion in the system. At later times, the connectivity is lost due to fragmentation of the network, and the long-time stretched exponential decay in the correlation function reflects the relaxation of clusters of various sizes.

Keywords: Hyaluronic acid; Chemical gelation; Degradation; Rheology; Dynamic light scattering

1. Introduction

Hyaluronan (sodium hyaluronate, hyaluronic acid, HA) is a linear anionic polysaccharide consisting of repeating disaccharide units of D-glucuronic and 2-acetamido-2-deoxy-D-glucose which are bound together by a β-(1→3)-type glucosidic bond. HA is one of the major components of the extracellular matrix of the connective tissues, and it is found in various locations such as synovial fluid, vitreous humor, skin, and umbilical cords. The high-molecular weight of HA together with its special viscoelastic features and biological functions has made HA as an attractive material to prepare biocompatible devices with applications in drug delivery and tissue engineering.[1–4] However, polymer matrices based on only HA are inclined in vivo to undergo a fast degradation by hyaluronidase.[1,3] In a recent dynamic light scattering investigation[5] on aqueous chitosan–gelatin mixtures in the presence of the enzyme tyrosinase, the formation and destruction of a transient gel was monitored.

To improve the mechanical properties of HA, the polymer chains are often chemically cross-linked by using different reactions to form a hydrogel.[3] Chemical agents such as divinyl sulfone, homobifunctional glycidyl ethers, bis(epoxides), glutaraldehyde, and formaldehyde have been utilized to cross-link HA chains in aqueous media under various conditions. In addition

* Corresponding author. Tel.: +47 22855508; fax: +47 22855441; e-mail: a.l.kjoniksen@kjemi.uio.no

0008-6215/$ - see front matter © 2007 Elsevier Ltd. All rights reserved.
doi:10.1016/j.carres.2007.08.021

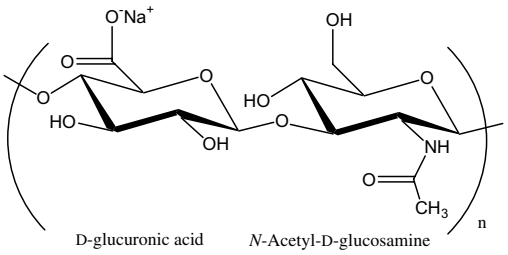

Sodium hyaluronate (Hyaluronic acid, HA)

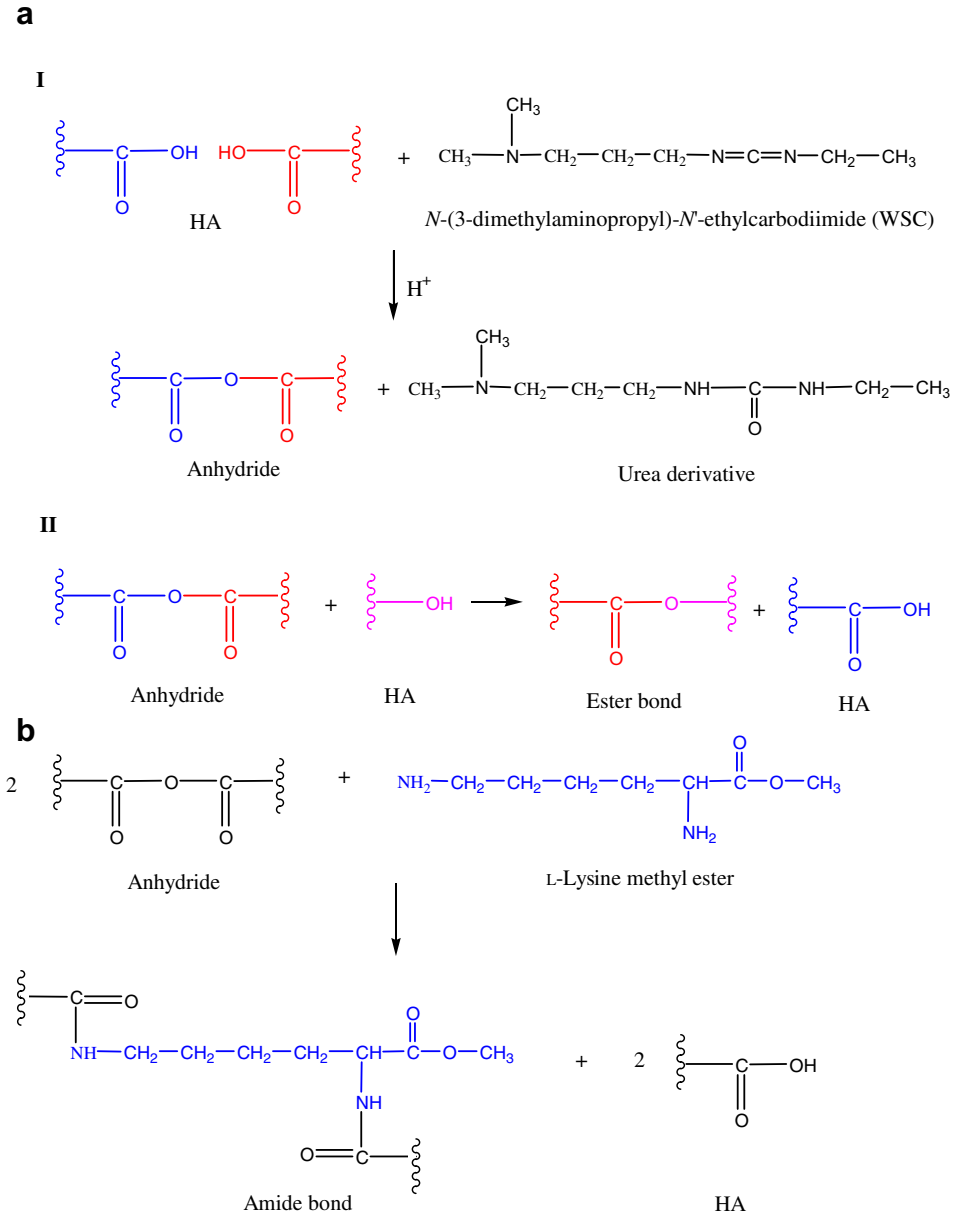

Chart 1. Reaction schemes for cross-linking of HA with different cross-linkers: (a) WSC (formation of anhydride and ester cross-linking bonds), (b) WSC in the presence of L-lysine methyl ester (addition of the lysine derivative results in the formation of intermolecular amide linkages in competition with the creation of ester bonds), and (c) Ugi multicomponent condensation reaction and the formation of amide linkages.

to these conventional cross-linker agents, HA has been chemically cross-linked[6,7] to form a hydrogel by using a water-soluble carbodiimide (WSC), which in contrast to conventional agents does not chemically bind to polysaccharide molecules.[8] It was suggested[7] that intermolecular formation of ester bonds between the hydroxyl

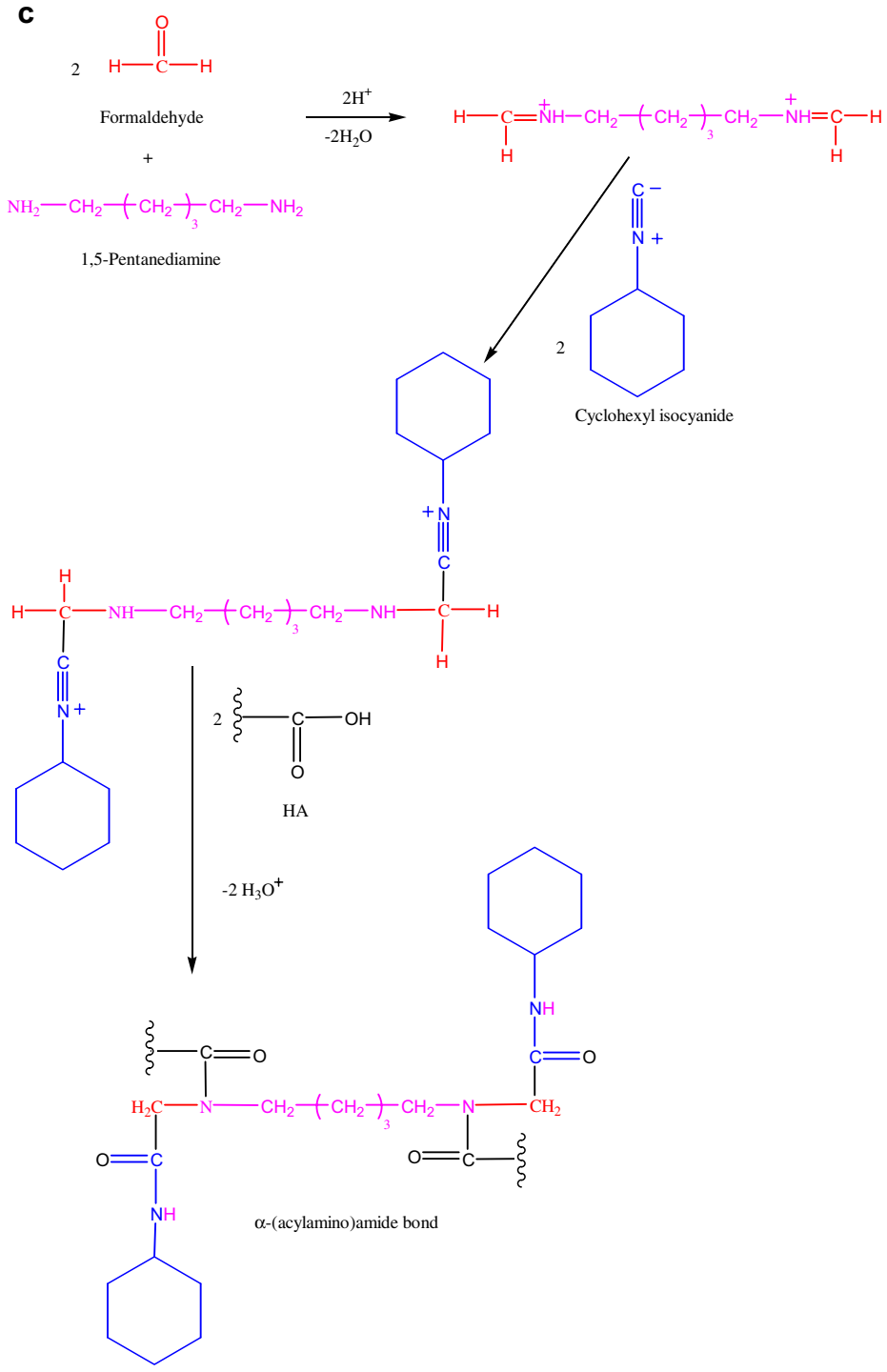

Chart 1 (*continued*)

and carboxyl groups belonging to different polysaccharide chains will induce cross-linking and the evolution of a gel network. However, ester bonds are known to be sensitive to hydrolysis, and to reduce this tendency of network disruption it has been found that the addition of L-lysine methyl ester with two amino groups in a molecule to the reaction medium containing WSC will suppress the hydrolytic degradation of the network.[7] It was argued[7] that in this case an amide bond is formed between the carboxyl group of a HA molecule and the amino group of L-lysine methyl ester. This type of bond is expected to have a higher resistance against degradation of the network. Another powerful method to cross-link carboxylated polysaccharide chains is via Ugi's multicomponent condensation reaction,[9] where the reaction mixture contains a diamine, which condenses with

the carbonyl group to yield an imine. The protonated imine and the carboxylate react with the isocyanide to give an α-(acylamino) amide (cf. Chart 1c). It has been shown in several studies[10–13] that, by using a bifunctional cross-linker, hydrogels with diamide linkages between polysaccharide chains are formed. The Ugi gels are known to be stable and the amide linkage is resistant to hydrolysis at alkaline conditions.

In the present work, we have carried out rheological and dynamic light scattering experiments to characterize the gelation process and the time-dependent degradation of the gel network when the samples are cross-linked with the WSC medium, with WSC in the presence of L-lysine methyl ester, or via the Ugi condensation reaction. The cross-linking schemes for the different reactions are schematically represented in Chart 1. When WSC is employed as a cross-linker agent for the HA chains at acid conditions, WSC induces intermolecular formation of an acid anhydride between two carboxyl groups, while WSC is transformed into a urea derivative. This anhydride is then responsible for the reaction with a hydroxyl group to yield an ester bond between adjacent polysaccharide chains.[7] If L-lysine methyl ester with two amino groups is added to the reaction medium containing WSC, the hypothesis is[7] that amide bonds are formed, which have higher resistance against hydrolytic degradation. By using the classical Ugi reaction, amide linkages are formed between the HA molecules.

In addition, the effect of pH on the cross-linking of HA with WSC will be examined and the hydrolytic degradation of HA will be probed with the aid of the asymmetric flow field-flow fractionation technique (AFFFF). The aim of this study is to acquire intimate knowledge of the rheological and dynamical features during the gelation process and the subsequent hydrolysis at different cross-linking conditions. This insight is important to tailor-made polymer systems for applications in, for example, controlled drug delivery. To the best of our knowledge, these issues have not been addressed in a systematic investigation before. Furthermore, we will provide some novel features about the dynamics during gelation and in the gel-breakage regime.

2. Experimental

2.1. Materials

In this work, a HA sample (sodium hyaluronate, Pharma grade 150; lot. no. 051106) was supplied by NovaMatrix, FMC BioPolymer, Drammen, Norway. The results from the AFFFF experiments showed[14] that the polymer sample has a weight-average molecular weight of $M_w = 1.9 \times 10^6$ and a narrow molecular weight distribution with a polydispersity index of $M_w/M_n = 1.1$ (see also Fig. 3). According to the manufacturer, the protein contents of the polymer are less than 0.1%.

Hydrochloric acid, sodium hydroxide, *N*-(3-dimethylaminopropyl)-*N*′-ethyl-carbodiimide hydrochloride (WSC), formaldehyde, 5-diaminopentane (DAP), and cyclohexyl isocyanide were purchased from E. Merck or Fluka and were of analytical grade. Citric acid and L-lysine methyl ester dihydrochloride salt (hereafter this compound is called L-lysineME) were obtained from Sigma–Aldrich. These chemicals were used without any further purification. Double distilled Millipore water was utilized in this work.

2.2. Preparation of solutions and gel formation

HA was dissolved in water and a homogeneous 0.5 wt % solution, which is well above the overlap concentration (semidilute regime), was prepared. When cross-linking occurs via the WSC procedure, this agent was added and allowed to dissolve and distribute homogeneously throughout the solution. In this work, different cross-linker concentrations (5 wt % (0.26 m), 10 wt % (0.52 m), and 16 wt % (0.83 m)) were employed. An aqueous solution of citric acid (1 wt %) was then added as catalyst[15] to the polymer solutions, in a 5 vol/vol amount (no gel formation was observed in the absence of the citric acid catalyst). The value of pH of the HA solution is approximately 5, but when the cross-linker agent is added and the reaction proceeds the value of pH is changed (see Fig. 1 and Table 1). In some cases when we wanted to study the effect of pH on the cross-linker process (cf. the discussion below), pH was adjusted to higher or lower values prior to the

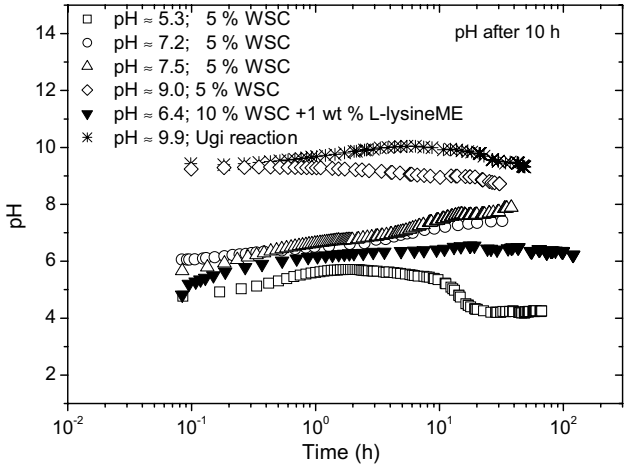

Figure 1. Illustration of the change of pH during the cross-linker reaction for a 0.5 wt % HA sample at various pH (the pH values indicated in the figure refer to the pH values of the reaction mixtures after 10 h) in the reaction mixtures of 5 wt % WSC and 0.05% citric acid, and with WSC in the presence of L-lysineME and for the Ugi condensation reaction.

Table 1. Characteristic parameters for incipient gels obtained for 0.5 wt % hyaluronic acid at different pH values (the pH values before adding the cross-linker agent and after 10 h of the cross-linking process are indicated) and cross-linker conditions

0.5 wt % HA 5 wt % CA	GP (min)	n
$pH_{start} \sim 3/pH_{10\,h} \sim 5.3$		
5 wt % WSC	118	0.58
$pH_{start} \sim 5/pH_{10\,h} \sim 7.2$		
5 wt % WSC	61	0.48
10 wt % WSC	43	0.56
16 wt % WSC	32	0.55
$pH_{start} \sim 8/pH_{10\,h} \sim 7.5$		
5 wt % WSC	67	0.53
$pH_{start} \sim 4/pH_{10\,h} \sim 6.4$		
10 wt % WSC 1 wt % L-LysineME	78	0.62
$pH_{start} \sim 4$		
10 wt % WSC 2 wt % L-LysineME	82	0.57
$pH_{start} \sim 3/pH_{10\,h} \sim 9.9$		
Ugi reaction 0.13 wt % Cross-linker	36	0.42

cross-linking reaction by adding 0.1 M NaOH or 4 M HCl dropwise to the solution under stirring. However, also at these conditions the values of pH are altered in the course of the cross-linker reaction (Fig. 1). Further aspects on the effect of pH on the cross-linker reactions are discussed below.

In some reactions with WSC, HA was dissolved in water containing (1 wt % (0.04 m) and 2 wt % (0.09 m)) L-lysineME before the WSC agent and citric acid were added as described above. As already mentioned, the intention with this procedure is to create some amide linkages between the polysaccharide chains that are more resistant to hydrolysis than ester bonds.

For the Ugi condensation reaction, the pH of the homogeneous HA solution was slightly adjusted by adding 1 drop of 4 M HCl to a value of approximately 3, which is necessary for the Ugi reaction to proceed,[11] and the polymer concentration was fixed at 0.5 wt %. Formaldehyde (2 μL/g), the bifunctional cross-linker 1,5-diaminopentane (1.5 μL/g), and cyclohexyl isocyanide (2 μL/g) were added to the solution successively, the resulting concentrations of these components were 0.06 m, 0.01 m, and 0.02 m, respectively. After the addition of each component, the solution was stirred vigorously to disperse the chemicals homogeneously in the solution. In these experiments, the cross-linker concentration was 0.13 wt %. The other components in the reaction mixture were added in excess. After the last component cyclohexyl isocyanide was added, the solution was stirred and then within a few minutes loaded in the rheometer. An illustration of possible cross-links formed by an Ugi reaction for HA is given in Chart 1. All measurements in this study were performed at 25 °C.

2.3. pH measurements

The pH values of the solutions and during the gelation process were determined by using a PHM210 standard pH meter (Radiometer Analytical S.A., France) at room temperature.

2.4. Rheology

Oscillatory sweep measurements were carried out in a Paar-Physica MCR 300 rheometer using a cone-and-plate geometry, with a cone angle of 1° and a diameter of 75 mm. The samples were carefully applied on the plate, and a thin layer of low-viscosity silicone oil was used to cover the free surface of the solution to prevent evaporation of solvent. No effect of the silicone oil on the physical properties of the samples could be detected, and the viscoelastic response of the sample is virtually not affected by this layer. The values of strain amplitude were checked to ensure that all measurements were conducted in the linear viscoelastic regime, where the dynamic storage modulus (G') and loss modulus (G'') are independent of the strain amplitude. The measurements were conducted over a broad angular frequency (ω) domain. The measuring device is equipped with a temperature unit (Peltier plate) that provides a good temperature control (25 ± 0.05 °C) over extended time.

2.5. Analysis of rheological results

The rheological behavior at the gel point of a polymer system can be described by a power law, where the dynamic moduli are related as[16]

$$G' = G''/\tan\delta = S\omega^n \Gamma(1-n)\cos\delta \qquad (1)$$

where $\Gamma(1-n)$ is the gamma function, n is the relaxation exponent, and S is the gel strength parameter, which depends on the cross-linking density and the chain flexibility.[16] The phase angle δ between stress and strain is independent of the angular frequency but proportional to the relaxation exponent

$$\tan\delta = G''/G' = \tan(n\pi/2) \qquad (2)$$

The following scaling relation can describe an incipient gel:

$$G'(\omega) \propto G''(\omega) \propto \omega^n \qquad (3)$$

However, if the dynamic moduli exhibit weak frequency dependence, it is expedient to probe the evolution of the rheological properties during gelation through the complex viscosity, with its absolute value $|\eta^*(\omega)|$ given by

$$|\eta^*(\omega)| = (G'^2 + G''^2)^{1/2}/\omega \qquad (4)$$

The frequency dependence of the absolute value of the complex viscosity at the gel point (GP) can be described in terms of a power law in angular frequency[17]

$$|\eta^*(\omega)| = aS\omega^{-m} \quad (5)$$

with

$$m = 1 - n \quad (6)$$

and

$$a = \frac{\pi}{\Gamma(n)\sin(n\pi)} \quad (7)$$

where m is related to the relaxation exponent n. We notice that if the frequency dependence of the dynamic moduli is weak (n is close to 0), a strong, easily detected dependency of m (m approaches 1) is expected. Values of m close to zero indicate liquid-like performance, whereas values of m approaching 1 suggest solid-like response.

The gel point is usually established by the observation of a frequency-independent value of $\tan\delta$ ($=G''/G'$) obtained from a multifrequency plot of $\tan\delta$ versus time.[18]

2.6. Asymmetric flow field-flow fractionation (AFFFF)

The AFFFF experiments were conducted on an AF2000 FOCUS system (Postnova Analytics, Landsberg, Germany) equipped with an RI detector (PN3140, Postnova) and a multiangle (seven detectors in the range 35–145°) light scattering detector (PN3070, $\lambda = 635$ nm, Postnova).

Before adding the cross-linker agent and the catalyst (citric acid), a 0.1 wt % HA solution in 0.01 M NaCl was characterized with the AFFFF instrument, whereas the samples studied at different times during the cross-linking process were measured using 0.5 wt % HA solutions with 0.05% citric acid and 5% WSC. All measurements were carried out using a 350 μm spacer, a regenerated cellulose membrane with a cutoff of 5000 (Z-MEM-AQU-426N, Postnova), and an injection volume of 20 μL.

The measurements of the HA solution without cross-linker agent were performed by employing a constant detector flow rate of 1 mL/min. The focusing time was 6 min at a cross-flow of 2 mL/min. Thereafter, the cross-flow was reduced exponentially (exponent of 0.2) to 0.1 mL/min during a 5 min period. The cross-flow was then linearly reduced to zero during a period of 10 min.

The experiments on the HA samples that had been cross-linked for 40 h or 7 days after start were performed by employing a constant detector flow rate of 0.2 mL/min and a slot-pump flow rate of 0.8 mL/min. The focusing time was 6 min at a cross-flow of 4 mL/min. Thereafter, the cross-flow was reduced exponentially (exponent of 0.2) to 0.1 mL/min during a 5 min period. The cross-flow was then linearly reduced to zero during a period of 15 min.

The measurements on the HA sample that had been cross-linked for 80 days were conducted by employing a constant detector flow rate of 0.2 mL/min, and a slot-pump flow rate of 0.8 mL/min. The focusing time was 4 min at a cross-flow of 3 mL/min. Thereafter, the cross-flow was reduced exponentially (exponent of 0.2) to 0.2 mL/min during a 5 min period. The cross-flow was then linearly reduced to zero during a period of 10 min.

Processing of the measured data was achieved by the Postnova software (AF2000 Control, version 1.1.011). The molecular weight and root-mean radius of gyration of the solutions were determined using this software with a random coil fit, and a refractive index increment (dn/dc) of 0.134 (determined by using the RI-detector at 32 °C).

2.7. Dynamic light scattering measurements (DLS)

The setup for the intensity and dynamic light scattering experiments is an ALV/CGS-8F multidetector version compact goniometer system, with 8 off fiber-optical detection units, from ALV-GmbH, Langen, Germany. The light source is a Uniphase cylindrical 22 mW HeNe-laser operating at a wavelength of 632.8 nm with vertically polarized light. The beam was focused on the sample cell (10-mm NMR tubes, Wilmad Glass Co., of highest quality) through a temperature-controlled cylindrical quartz container (with two plane-parallel windows), vat (the temperature constancy being controlled to within ±0.01 °C with a heating/cooling circulator), which is filled with a refractive index matching liquid (*cis*-decalin). The sample solutions were filtered in an atmosphere of filtered air through, depending on the viscosity of the solution, 0.8- or 5-μm filters (Millipore) directly into precleaned NMR tubes.

The light scattering process defines a wave vector $q = (4\pi n/\lambda)\sin(\theta/2)$, where λ is the wavelength of the incident light in a vacuum, θ is the scattering angle, and n is the refractive index of the medium. The refractive index (at 25 °C) was measured with an automatic refractometer (model PTR 46) purchased from Index Instruments Ltd., England. The temperature of the instrument is controlled electronically to a high stability by using a Peltier cell.

The full homodyne intensity autocorrelation function was measured at eight scattering angles simultaneously in the range 17–136° with four ALV 5000/E multiple-τ digital correlators. If the scattered field obeys Gaussian statistics, the measured correlation function $g^2(q,t)$ can be related to the theoretically amenable first-order electric field correlation function $g^1(q,t)$ by the Siegert relationship[19] $g^2(q,t) = 1 + B|g^1(q,t)|^2$, where B is usually treated as an empirical factor. No reduction of the initial

amplitude of the correlation function during the gelation process could be detected, and no other signs of non-ergodicity was found for the samples considered in this work.

2.8. Analysis of the dynamic light scattering data

Several DLS studies[20–23] on complex polymer systems have revealed the existence of two relaxation modes. The picture that emerges from this investigation is that the decay of the correlation function for gel-like systems can initially be described by a Kohlrausch–Williams–Watts[24,25] stretched exponential, followed at longer times by a power law,[20] whereas for solutions the correlation function can be fitted with the aid of a double stretched exponential. We have analyzed the correlation data by using the following relationships

$$g^{(1)}(t) = A_f \exp\left[-\left(\frac{t}{\tau_{fe}}\right)^{\beta_f}\right] + \frac{A_s}{\left(1+\frac{t}{V}\right)^d} \quad (8a)$$

$$g^{(1)}(t) = A_f \exp\left[-\left(\frac{t}{\tau_{fe}}\right)^{\beta_f}\right] + A_s \exp\left[-\left(\frac{t}{\tau_{se}}\right)^{\beta_s}\right] \quad (8b)$$

with $A_f + A_s = 1$. The parameters A_f and A_s are the amplitudes for the fast and the slow relaxation modes, respectively. Analyses of the time correlation functions of the concentration fluctuations at long wavelengths in the semidilute concentration regime have shown that the first term (short-time behavior) on the right-hand side of Eqs 8a and 8b is related to a mutual diffusion coefficient D_m ($\tau_f^{-1} = D_m q^2$) or a cooperative diffusion coefficient D_c in the semidilute concentration regime. The variable V in Eq 8a is the time at which the power-law tail begins,[20] and d is the power-law exponent. The power-law behavior described by the second term in Eq 8a is a feature that is usually reported[20,26–31] for gelling systems. The second term in Eq 8b (long-time feature) is associated with disengagement relaxation of individual chains or cluster relaxation.[32] The variables τ_{fe} and τ_{se} are some effective relaxation times, and β_f ($0 < \beta_f \leqslant 1$) and β_s ($0 < \beta_s \leqslant 1$) measure the widths of the distributions of relaxation times. The mean relaxation times are given by

$$\tau_f \equiv \int_0^\infty \exp[-(t/\tau_{fe})^{\beta_f}]dt = (\tau_{fe}/\beta_f)\Gamma(1/\beta_f) \quad (9a)$$

$$\tau_s \equiv \int_0^\infty \exp[-(t/\tau_{se})^{\beta_s}]dt = (\tau_{se}/\beta_s)\Gamma(1/\beta_s) \quad (9b)$$

where Γ is the gamma function.

In the analysis of the correlation function data, a nonlinear fitting algorithm (a modified Levenberg–Marquardt method) was utilized to best-fit values of the parameters appearing on the right-hand side of Eq 8a or 8b. The values of β_f determined in this study were always close to 1 ($\beta_f \approx 0.9$), but to account for polydispersity effects, this parameter was allowed to float in the fitting process.

3. Results and discussion

3.1. Rheological properties

We will start this discussion by showing how the viscosities of the systems change in the course of the cross-linker process for the different samples, and then the characteristic properties of the incipient gels will be analyzed. Time evolution of the absolute value of the complex viscosity (at a constant angular frequency of 1 rad/s) during gelation of a 0.5 wt % HA solution (with 0.05 wt % citric acid) at different cross-linker densities is depicted in Figure 2a, together with a HA sample containing 10 wt % WSC in the presence of different concentrations of L-lysineME. The general trend for all systems is the growth of $|\eta^*|$ as the gelation proceeds and the increase continues beyond the gel point. However, we note that after some time $|\eta^*|$ passes through a maximum and the value of $|\eta^*|$ drops considerably

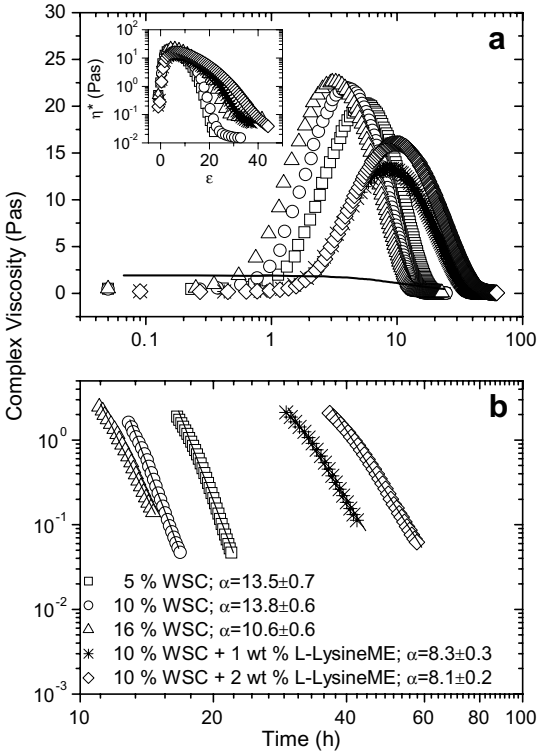

Figure 2. (a) Time evolution of the absolute value of complex viscosity (constant angular frequency of 1 rad/s) for a fixed HA concentration of 0.5 wt % with 0.05 wt % citric acid at different cross-linker concentrations, with and without added L-lysineME. The solid line shows the data for 0.5 wt % HA with 0.05 wt % citric acid without any cross-linker present. (b) Quantitative illustration of the kinetics for the breakdown of the network at long times (after the complex viscosity maximum) in terms of a power law ($|\eta^*| \sim t^{-\alpha}$).

as time goes. This peculiar feature can be rationalized in the following way. The value of $|\eta^*|$ is governed by the ubiquitous competition between the interpolymer chemical cross-linking of the HA chains and the degradation of the polymer due to hydrolysis[3,7] of the bonds. It is well known that ester linkages can be hydrolyzed under both acid and basic conditions. In addition, as is discussed below, the glycosidic bonds may be broken up. In the beginning, the cross-linking of the polymer chains dominates, but as the cross-linker agent is consumed, the breaking down of bonds of the polymer prevails and this leads to disruption of the network. We notice that the amplitude of the viscosity peak is higher at a higher cross-linker concentration, and the peak maximum is shifted toward shorter time. The reason is that a higher cross-linker concentration promotes a faster growth of the network, but at the same time, a larger number of ester bonds will also facilitate the commencement of the hydrolysis. For a 0.5 wt % HA solution with 0.05 wt % citric acid without any cross-linker present (solid line in Fig. 2a), a slight viscosity decrease was observed. The viscosity at long times is lower for the samples containing the WSC cross-linker than for the sample without the cross-linker.

The effect of addition of L-lysineME with two amino groups in a molecule to the reaction medium containing WSC is to suppress the hydrolysis. The idea behind this action is that some stable amide bonds[7,8] should be formed, and thereby the gel networks should have higher resistance against hydrolytic degradation than those cross-linked through ester bonds alone. Although the hydrolysis is delayed, it does not seem to prevent a severe breakdown and fragmentation of the network. An increase of the L-lysineME concentration has only a marginal effect on the viscosity, with somewhat higher values of $|\eta^*|$ around the maximum. In the inset, $|\eta^*|$ is plotted versus ε (where $\varepsilon = (t - t_{GP})/t_{GP}$ is the relative distance from the gel point t_{GP}) for the systems depicted in Figure 2a. The fact that the viscosity peaks by this procedure are located at approximately the same value of ε suggests that the difference in peak position observed in Figure 2a can be ascribed to different times of gelation for the studied systems (cf. Table 1). The inset is plotted with a logarithmic y-axis to illuminate the changes in the low-viscosity range. The viscosities at long times are clearly much lower than the initial viscosities, which indicates that the viscosity decrease is not only due to the breaking up of the cross-linking bonds.

Figure 2b shows a log–log plot of $|\eta^*|$ (after the maximum) as a function of time to gain a more quantitative insight into the kinetics of the breakdown of the gel network. After the maximum, the time evolution of $|\eta^*|$ can be described by a power law $|\eta^*| \sim t^{-\alpha}$, where α is a power-law exponent. We note that a higher cross-linker density with WSC favors a faster degradation, probably because more ester bonds are available for hydrolysis. Addition of L-lysineME to the reaction medium slows down the rate of the hydrolytic degradation, which is assigned to the formation of amide bonds.

At this point, it is important to investigate whether the hydrolysis only affects the ester linkages, or if the glycosidic bonds of the polymer backbone are also broken up and thereby the molecular weight of the polymer is reduced. The asymmetric flow field-flow fractionation is a powerful technique to monitor the degradation of HA in the course of the cross-linking process with WSC. By this method, we can probe how the molecular weight and molecular weight distribution of the polymer change as the hydrolysis proceeds over a long period. At this stage, the pH of the solution is approximately 7. In Figure 3, results from AFFFF measurements over a long time for 0.5 wt % HA with 0.05 wt % citric acid, without cross-linker and with with 5 wt % WSC, are displayed. Prior to cross-linking, the weight-average molecular weight of HA is high ($M_w = 1.9 \times 10^6$) and the

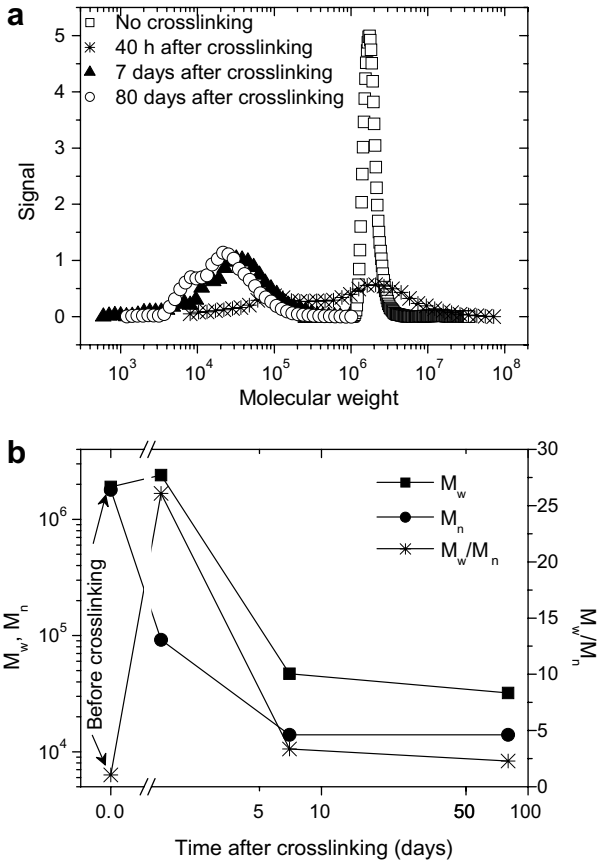

Figure 3. (a) Molecular weight distribution for a fixed HA concentration of 0.5 wt % with 0.05 wt % citric acid without cross-linker and in the presence of 5 wt % WSC at different stages during the hydrolysis (pH ≈ 7). (b) Plot of M_n, M_w, and the polydispersity index as a function of time after cross-linking.

molecular weight distribution is narrow ($M_w/M_n = 1.1$; M_n is the number average molecular weight). It is not possible to measure AFFFF during the gel formation due to the high viscosity and the ultrahigh-molecular weight of the cross-linked sample. About 40 h after the cross-linking process was started, M_w has increased to 2.4×10^6, while the value of M_n is drastically lower than before (9.2×10^4). This illustrates the competition between the cross-linking reaction (increasing molecular weight, as is obvious from M_w) and degradation (decreasing molecular weight, causing a reduction in M_n), resulting in an extremely polydisperse sample ($M_w/M_n = 26$). As time goes the cross-linked sample is disrupted and the reaction mixture contains large cross-linked clusters and degraded polymer, yielding a broad molecular weight distribution (maximum value of the polydispersity index). After several days, most of the ester linkages have been hydrolyzed, and the low-molecular weight-averages signalize severe rupture of the polymer chains. This indicates cleavage of glycosidic bonds of the polymer backbone in the course of time. The picture that emerges from these findings is that there are two simultaneous processes in the breaking down of the sample, namely hydrolysis of ester linkages and the scission of the polymer chains via glycosidic bonds. It should be noted that no degradation is observed for the HA sample without cross-linker agent.[14] Our conjecture is that ester linkages are hydrolyzed and the network structure is broken; the glycosidic bonds in the polymer backbone may be hydrolyzed as well under acetic conditions. This finding shows that besides the rupture of ester linkages, leading to fragmentation of the network, scission of the glycosidic linkages gives rise to a degradation of the polymer with a lower molecular weight. At present, we do not have a mechanism to describe the hydrolysis phenomena, but molecular weight reduction of the polymer is only observed in the presence of WSC.

The frequency dependencies of the absolute value of the complex viscosity, as measured in small amplitude oscillatory shear experiments, at different stages during the gelation process for a 0.5 wt % HA solution at different cross-linker concentrations are displayed in Figure 4. At all conditions, the frequency dependence of $|\eta^*|$ can be described by a power law $|\eta^*| \sim \omega^{-m}$. The general trend observed at all levels of cross-linker addition is that at early stages in the pregel domain, weak frequency dependence of $|\eta^*|$ is found (liquid-like behavior), whereas as the gel evolves, a progressively stronger dependence is observed during a certain period of time and a solid-like response is approached. However, at very long times, in contrast to many other chemical gels, the value of m falls off and the elastic response of the system is weakened.

It is generally assumed that when polysaccharides are chemically cross-linked with WSC to produce gels, basic

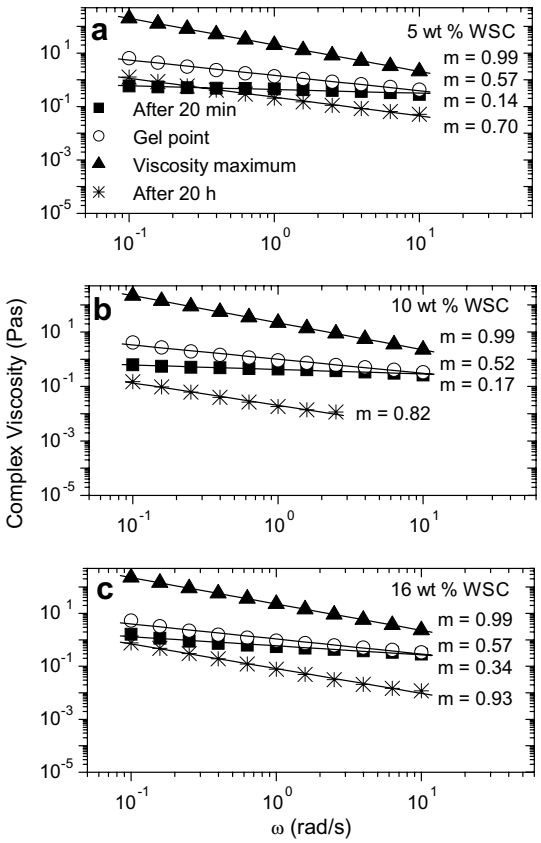

Figure 4. Frequency dependence of $|\eta^*|$ (log–log plot) at different stages during the gelation process for 0.5 wt % samples of HA with 0.05 wt % citric acid in the presence of the cross-linker concentrations indicated.

pH values promote hydrolysis of ester bonds. To investigate the effect of pH on the gelation process and degradation of the polymer network, we have prepared HA solutions with various pH values, covering an extended range (pH 3–12). The pH of the HA solutions without cross-linker was adjusted by adding a few drops of HCl or NaOH. The pH values of the reaction media are altered when WSC is added, and pH is changed as the cross-linker reaction proceeds (Fig. 1). Addition of WSC to HA solutions in the acid pH range increases the pH value, whereas the opposite trend is observed in HA solutions adjusted to a strongly basic pH. During the cross-linker reaction with WSC at pH 3–8, a moderate rise of pH can be traced, which may be ascribed to the formation of urea derivative (cf. Chart 1). At some conditions, the value of pH decreases at long times and this tendency may be due to the release of HA moieties. This effect is evident for the HA solution with the highest pH (pH $\approx$ 12), where no gel is formed during the cross-linker reaction. In the Ugi reaction, the amino groups yield a basic pH of the reaction medium and as HA chains are cross-linked, the pH of the reaction mixture increases somewhat. The slight decrease of pH at long times may be attributed to the hydrolysis of some

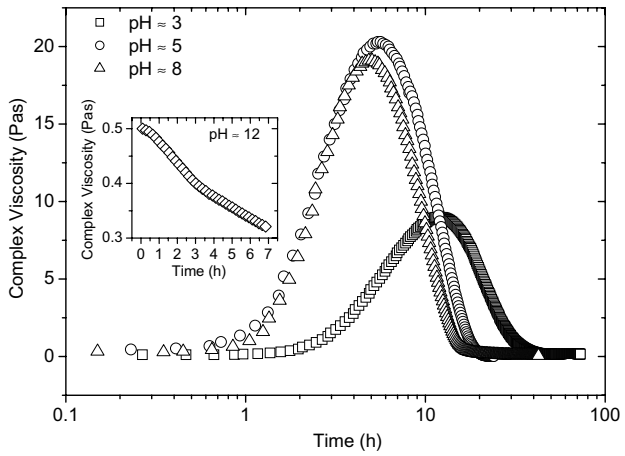

Figure 5. Time evolution of the absolute value of complex viscosity (constant angular frequency of 1 rad/s) for a fixed HA concentration of 0.5 wt % with 0.05 wt % citric acid in the presence of 5 wt % WSC at the pH values indicated. The inset shows the time evolution of the complex viscosity at a high pH where no gel is formed. The pH data refer to the adjusted values of the solutions prior to the addition of citric acid and the cross-linker agent.

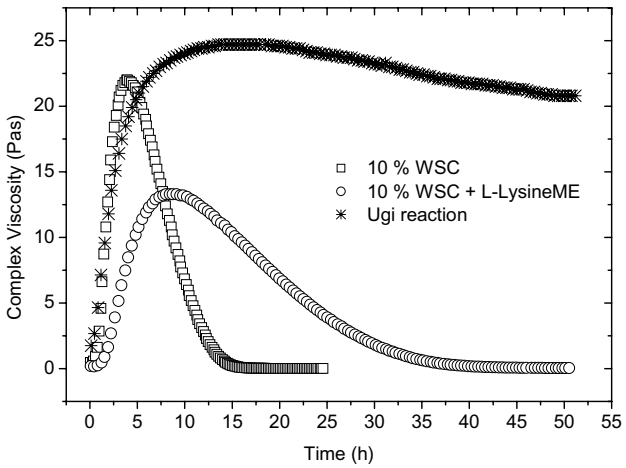

Figure 6. Time evolution of the absolute value of the complex viscosity (constant angular frequency of 1 rad/s) during the gelation process of 0.5 wt % HA with 0.05 wt % citric acid and 10 wt % WSC, with and without the addition of 1 wt % L-lysineME, and with 0.13 wt % cross-linker agent for the Ugi four-component condensation reaction.

ester linkages formed by the concomitant Passerini condensation reaction.[9]

The time evolution of $|\eta^*|$ at different pH values for reaction mixtures of 0.5 wt % HA with 0.05% citric acid in the presence of 5 wt % WSC is shown in Figure 5. Prior to the addition of the cross-linker, the pH of the solution was adjusted to the indicated values. At the highest pH value (pH $\approx$ 12), no gelation occurs and $|\eta^*|$ decreases monotonously in the course of time (see the inset plot). The reason for this behavior is that at this strongly basic condition, hydrolysis of glycosidic bonds occurs and the possible interpolymer cross-linker reaction is sturdily suppressed. At pH values of approximately 5 and 8, $|\eta^*|$ passes through a pronounced maximum (a significantly lower value of the viscosity maximum is observed at pH $\approx$ 3) before the hydrolytic degradation of the polymer dominates the process. This finding suggests that more interchain cross-links are favored by the higher pH values, but at the same time, the higher number of ester linkages will also accelerate the hydrolysis and this will lead to a faster disruption of the network (cf. Fig. 5). These results demonstrate that the value of pH plays an important role for the gelation process and the subsequent hydrolytic degradation of the polymer. We should note that even at the lowest pH value, hydrolysis takes place but it starts later and it takes longer time for the network to be broken up.

A comparison of the time evolution of $|\eta^*|$ during gelation and gel breakage for a fixed HA concentration of 0.5 wt % in the presence of 10 wt % WSC, with and without L-lysineME, and via the Ugi multicomponent condensation reaction for the same polymer concentration is presented in Figure 6. For the systems cross-linked with WSC, it is evident that the addition of L-lysine methyl ester to the reaction medium gives rise to weaker intermolecular formations but to a more resistant network against hydrolysis than that cross-linked with ester bonds alone. These results indicate that more interpolymer cross-links are formed in the absence of the L-lysineME and thereby a stronger network is built, but at the same time the reaction medium containing L-lysineME can produce a network connected by some amide linkages, which have higher resistance against hydrolysis. As a result, the breakdown of the network is postponed. We should remember that even when the reaction mixture contains L-lysineME, there is a continuous competition between the process yielding amide linkages and the concomitant reaction producing ester linkages.

The Ugi gelation reaction yields a gel network that exhibits a moderate degradation as time goes. In the Ugi four-component condensation the reaction mixture contains a diamine, which condenses with the carbonyl to yield an imine. The protonated imine and the carboxylate react with the isocyanide to give an α-(acylamino) amide (see Chart 1c). In this process, diamide linkages are formed between the polysaccharide chains and these linkages are known[10] to be resistant against hydrolysis, in contrast to ester linkages that can be easily hydrolyzed (Chart 1a) over a broad pH range. In a reaction medium with WSC, where L-lysineME has been added, a polymer network is formed that consists partly of amide and partly of ester linkages (Chart 1b). The moderate decrease of $|\eta^*|$ over time for the Ugi gel may suggest that some ester bonds possibly formed by the parallel Passerini condensation reaction were broken, but even after a long time (more than several weeks) the sample is still a gel.

3.2. Properties of incipient gels

When gelling samples are characterized, rheological features of the incipient gels yield important information about the systems. In the approach of Winter and Chambon,[18] the gel point can be determined by observation of a frequency-independent value of $\tan\delta$ ($=G''/G'$) obtained from a multifrequency plot of $\tan\delta$ versus time. Typical illustrations of gelation for a 0.5 wt % solution of HA in the presence of 10 wt % WSC, or with the Ugi condensation reaction, are depicted in Figure 7. The common feature observed for all gelling systems presented in Table 1 is that the loss tangent is frequency dependent and decreases during gel formation, indicating that the systems become more and more elastic (cf. Fig. 7). The time of gelation is identified at the point where a frequency-independent value of the loss tangent is observed. At the gel point, G' and G'' curves become parallel to each other, and a power-law behavior is observed over an extended frequency domain (see the insets of Fig. 7). For some incipient gels we observe that $G'' < G'$, whereas for other systems $G'' > G'$. For instance, in the insets in Figure 7 we note that $G'' > G'$ for HA with 10 wt % WSC and $G'' < G'$ for the Ugi gel. At the gel point, it is usually observed[33–36] for 'strong' chemical gels that $G'' > G'$, while for 'weak' gels $G'' < G'$ has been reported.[37,38]

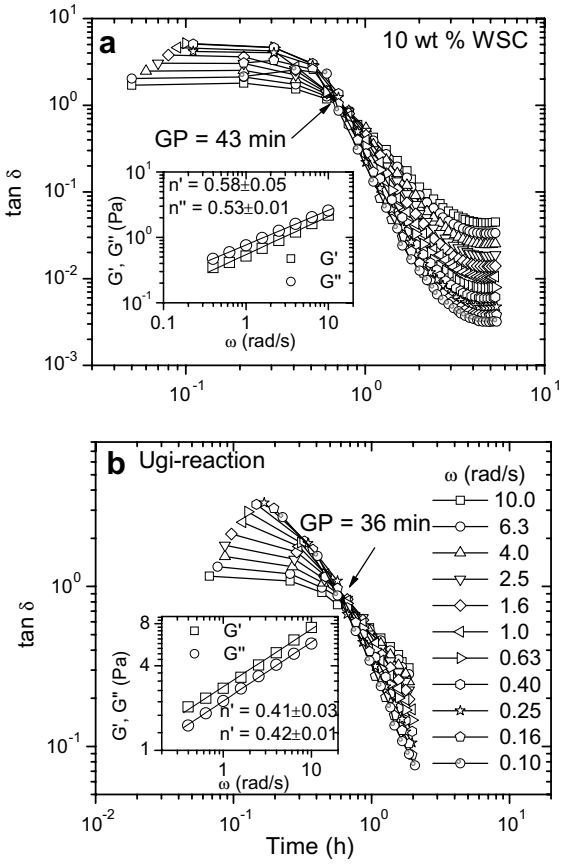

Figure 7. Viscoelastic loss tangent as a function of time for the frequencies indicated during the cross-linking process of 0.5 wt % of HA in the presence of 10 wt % WSC and 0.05 wt % citric acid (a) or with the Ugi condensation reaction with 0.13 wt % cross-linker agent (b). The gel points (GP) are indicated. The insets display plots of G' and G'' versus frequency for the systems at the gel point, showing the power-law behavior.

Some characteristic results of incipient gels, prepared at different conditions, are presented in Table 1. The main results can be summarized in the following way: (i) At a given pH, the time of gelation decreases with increasing amount of cross-linking agent, because the probability of forming interpolymer linkages with the cross-linker in the system increases. (ii) A low pH in HA solutions containing WSC seems to give rise to long gelation times, which is attributed to the pronounced hydrolysis at low pH and this reduces the rate at which interpolymer ester linkages are formed. (iii) At pH of approximately 5, addition of L-lysineME to the reaction medium containing WSC prolongs the gelation time, which reflects the competition between the formation of ester bonds and amide linkages. Although amide linkages are created, the result suggests that the number of them is not sufficient to impede the fragmentation of the network. (iv) It is interesting to note that in spite of the low cross-linker concentration, the Ugi reaction produces an incipient gel during a short period of time, which suggests that the Ugi cross-linker reaction is an efficient and fast process. (v) The values of the power-law exponent n are between 0.4 and 0.6 for the investigated systems. The formation of incipient gels is often interpreted in the framework of the percolation model[39,40], which describes the fraction of chemical bonds at the gel point to establish the connectivity of a sample-spanning cluster. This model predicts a value of $n = 0.7$, and this value has previously been reported for some chemically cross-linked polysaccharides. The reason for the lower values observed in this study can probably be traced to entanglement effects.[13,35,41] Because of the high-molecular weight of HA and its extended structure, entanglements are easily established at this concentration.[14]

3.3. Dynamic light scattering (DLS)

DLS is a powerful technique to probe relaxation processes in gelling polymer systems and to gain insight into the dynamics. To illustrate this, we have carried out DLS experiments on 0.5 wt % HA samples (with 0.05 wt % citric acid) both without and with 5 wt % cross-linker agent. The results are shown in Figure 8, where the normalized time correlation data for a 0.5 wt % HA solution and a gelling 0.5 wt % HA sample at various stages are depicted in the form of a log–log plot. By checking the dependence of the decay curves of the time correlation function on the scattering

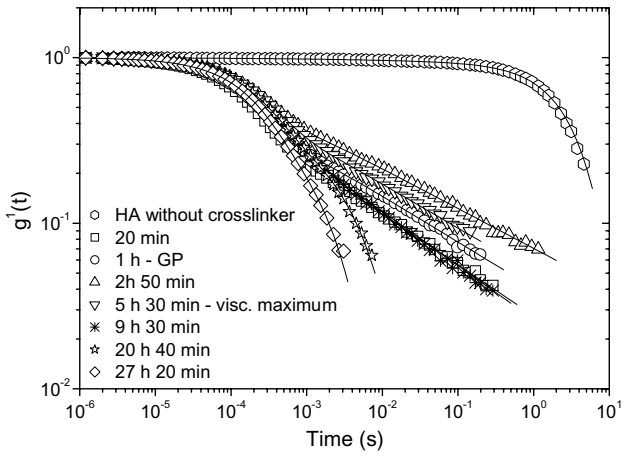

Figure 8. Time evolution of the first-order electric field correlation function (at a scattering angle of 85°) for 0.5 wt % of HA in the presence of 0.05 wt % citric acid and at different stages during the cross-linking process with 5 wt % WSC. Every 2nd point is shown. The solid curves are fitted with the aid of Eq 8a or 8b, depending on the profile of the decay.

position of the incident light in the sample, no nonergodic features could be traced for any of the systems reported in this work, and the samples were optically clear. This suggests that the scattering elements, although localized, exhibit sufficiently large displacements so that the scattered field can be considered as a zero-mean complex Gaussian variable. The reason why we have not detected any nonergodic signs of these chemically cross-linked systems may be that the interplay between the evolution of chemical cross-linking zones and the omnipresence hydrolysis of glycosidic bonds and ester linkages prevents the appearance of frozen-in fluctuations. At gelling conditions, the correlation functions representing stages not too far from the gelation point can be well described by an initial stretched exponential, followed by a power law in time at long times (cf. Eq 8a). The general trend is that the power-law tail is shifted toward longer times as the viscosity maximum is approached (cf. Fig. 2). However, beyond this maximum, the relaxation process becomes gradually faster, and at a late stage of the gel-breakage regime, the profile of the correlation function is changed and the decay can be portrayed by the sum of two stretched exponentials (see Eq 8b). A conspicuous feature in Figure 8 is the very slow decay of the relaxation process for the 0.5 wt % HA sample without cross-linker. At this scattering angle (85°), the correlation function can be described by the sum of two stretched exponentials. This slow relaxation is attributed to the enhanced entanglement situation in the solution of this high-molecular weight polymer. At this condition without added cross-linker, no degradation of the polymer has been detected over a long time. Usually when the polymer is chemically cross-linked, the decay of the correlation function is shifted toward longer times as the gel is formed. However, for the present system a divergent scenario emerges in the course of time. When the cross-linker is added to the HA solution, a continuous competition between interpolymer cross-linking of the polymer chains and hydrolysis of ester linkages and glycosidic bonds evolves directly, and this leads to disengagement of polymer chains and a faster relaxation.

The appearance of a power-law mark in the correlation function has been reported for many gelling systems around the gel point, and it has been suggested[20,26,27,30,31,42] that this feature is a signature of nonergodicity of the system. However, DLS studies[28,29,43] on nongelling systems have also disclosed power-law behavior of the relaxation mode at long time. In some DLS investigations[20,26,27] on gelling polymer systems, the power-law decay at long times is terminated by a stretched exponential. However, in this work the long-time tail was close to the base line and 'noise' in the DLS data appeared at this stage, and it was not possible to detect a long-time stretched exponential.

A power-law feature in the correlation function indicates a fractal time set[20] in the scattered field and the formation of a fractal-like hierarchical structure and the suppression of translational diffusion of clusters. The power-law decay suggests an absence of a finite characteristic time scale for the system, and the process is characterized by a continuous spectrum of relaxation times. In the theoretical model[44] by Doi and Onuki, the existence of a power-law regime in the decay of the correlation function was predicted. In some DLS studies[27,29,43] the power-law feature has been explained in terms of anomalous diffusion.

Figure 9a shows the time evolution of the fast relaxation time τ_f in the course of formation and breakage of the gel system discussed in Figure 8. In the time window before the gel point and well beyond the viscosity maximum, the correlation functions can be portrayed by means of Eq 8a (the sum of a stretched exponential and a power law) and τ_f can be calculated (see Eq 9a). The general trend is that τ_f rises and reaches a maximum when the interpolymer cross-linking behavior is dominant, followed by a decrease of τ_f during the stage of destruction of the gel. At a late phase of the gel-breakage regime, the long-time tail of the correlation function exhibits no longer a power-law profile but is transformed into a stretched exponential that is depicted by the second term on the right-hand side of Eq 8b. In this case, the initial decay of the correlation function is described by the first term on the right-hand side of Eq 8b (see the solid symbols in Fig. 9a). We observe large scatter in the DLS data presented in Figures 9–11, and the reason for this is the simultaneous building up and breaking down of the polymer network in the course of the cross-linking process. A similar trend

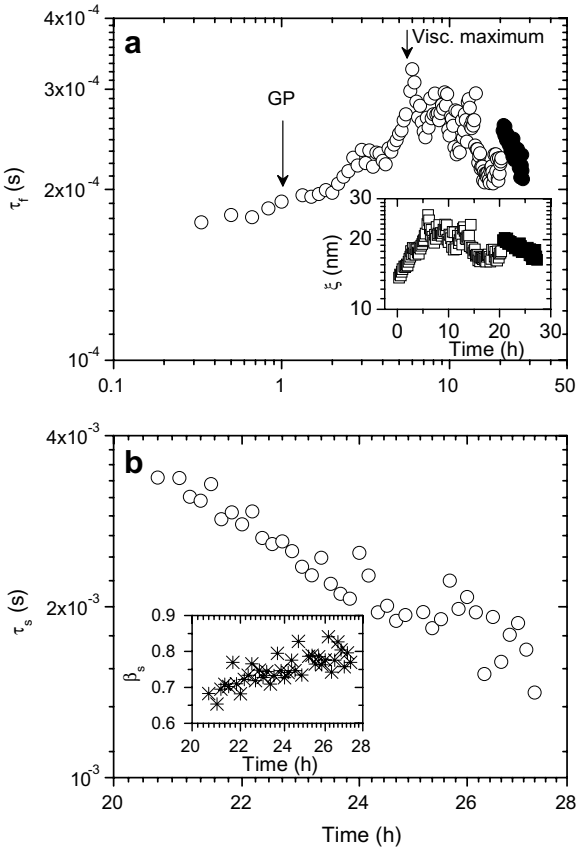

Figure 9. Time evolution of (a) the fast relaxation time, calculated from Eq 8a in combination with Eq 9a or from Eq 8b in combination with Eq 9b (solid symbols); the inset plot shows the correlation length versus time (see Eq 10) and (b) the slow relaxation time (calculated with the aid of Eq 8b in combination with Eq 9b) in the very late gel-breakage stage for 0.5 wt % HA in the presence of 5 wt % WSC. The inset plot shows the time dependence of the stretched exponent β_s.

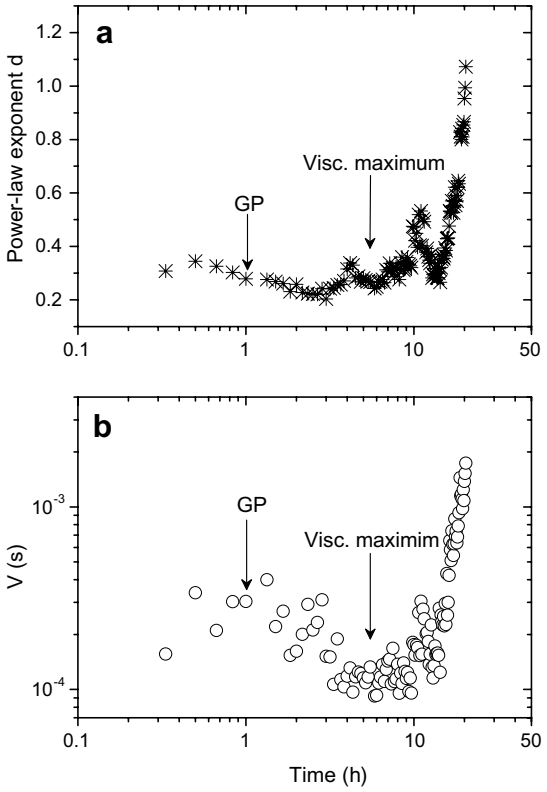

Figure 10. Time evolution of (a) the power-law exponent d and (b) the short-time cutoff of the power-law tail V; both parameters were obtained by fitting Eq 8a to the correlation functions for 0.5 wt % HA in the presence of 5 wt % WSC during the cross-linker process (see text for details).

can be seen in the DLS data obtained from the formation and destruction of chitosan–gelatin gels by the enzyme tyrosinase.[5]

The fast relaxation mode is always diffusive (see the discussion below) and in the framework of the blob model[39] in the semidilute concentration regime, the network dynamics can be characterized by the cooperative diffusion coefficient D_c ($\tau_f^{-1} = D_c q^2$) through the following expression:

$$D_c \cong \frac{k_B T}{6\pi\eta\xi} \tag{10}$$

where k_B is the Boltzmann constant, ξ is the correlation length or the average mesh size of the network, and η is the viscosity of the solvent at temperature T. Time evolution of ξ is illustrated in the inset of Figure 9a, and the rise of ξ may be that interpolymer cross-linking of chains gives rise to a reorganization of the network to a more heterogeneous one with a larger average mesh size. This type of behavior has been reported[23,36] for other gelling polymer systems. The drop of ξ in the inset at late time probably reflects a reorganization of the network to a more homogeneous one as the cross-linking zones are disintegrated. It has been argued[45] that the degree of nonuniformity of the network structure can play a role in the diffusion properties. This approach predicts an increase of the value of the diffusion coefficient or a decrease of the value of τ_f (Fig. 9a) with decreasing nonuniformity. It is reasonable to assume that a more homogeneous network is developed when the cross-linking zones of intertwined chains are disrupted.

At a very late stage of the hydrolysis of the polymer (the long-time tail of the correlation function is described by a stretched exponential; Eq 8b), the network is strongly fragmented and the blob approach with a mesh size ξ is no longer a relevant framework for the analysis of the fast relaxation mode. Anyhow, the drop of τ_f at late time (solid symbols in Fig. 9a) suggests that the value of the diffusion coefficient increases as the disruption of the network continues. This is expected because the steady breakage of ester linkages and scission of chains during the hydrolysis will produce small polymer species with high values of the diffusion coefficient.

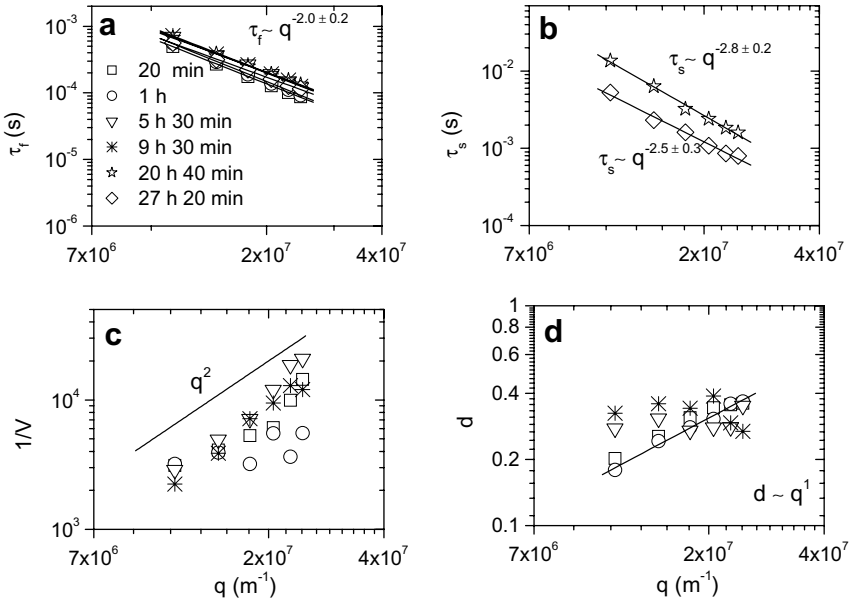

Figure 11. Angular dependences of the fast relaxation time (τ_f), of the slow relaxation time (τ_s) (Eqs 8b and 9), of the short-time cutoff of the power-law tail V (Eq 8a), and the power-law exponent d (Eq 8a) for 0.5 wt % HA in the presence of 5 wt % WSC during the cross-linker process (see text for details).

The time dependences of the slow relaxation time (τ_s) and the stretched exponent (β_s) in the late stage of gel breakage (Eq 8b) are displayed in Figure 9b. The value of τ_s falls off as the polymer network breakdowns during the hydrolysis. This trend is expected because the gradual disruption of the network and disengagement of polymer chains should promote faster relaxation of polymer species. The increase of β_s in the course of the degradation process of the sample suggests that the distribution of relaxation times becomes narrower. This finding suggests that the size distribution of the relaxing entities becomes smaller. It is expected that the continuous hydrolysis will lead to the breakup of large clusters in the reaction mixture, and produce species with a less broad size distribution.

Let us now discuss some characteristic features obtained from the analysis of the power-law tails of the correlation functions with the aid of Eq 8a. The time development of the power-law exponent d in the course of the formation and destruction of the gel is depicted in Figure 10a. The general tendency is that the value of the power-law exponent d decreases as the viscosity maximum is approached, and during the breakup of the gel, d exhibits a steep rise. These results may be rationalized in the framework of a model based on anomalous diffusion.[27] In ordinary diffusion the mean square displacement $\langle x^2 \rangle$ is given by $\langle x^2 \rangle = 2Dt$, whereas anomalous diffusion[46] may be described by a relationship of the type $\langle x^2(t) \rangle \propto t^b$ with $b < 1$, which represents a generalization of the Einstein equation. In disordered systems correlated motion may occur, and this type of memory effect may give rise to anomalous diffusion or fractal diffusion.[47,48] The slowing down of the diffusion motion is caused by the delay of a diffusing unit because of a hierarchically intricate structure. This situation may arise in gelling polymer systems, where the formation of regions of enhanced and reduced chain densities and decreased chain mobility due to cross-links may lead to anomalous diffusion. In a previous pulsed field gradient nuclear magnetic resonance (PFG NMR) study[49] on gelling aqueous solutions of poly(ethylene oxide)–poly(propylene oxide)–poly(ethylene oxide) block copolymer (Pluronic) the value of b was observed to drop as the gelation process proceeded, and b was found to be about 0.5 in the gel zone. It has been argued[27,29,43] that the power-law tail in the correlation function is related to anomalous diffusion. In view of this, the decrease of d in the region up to the viscosity maximum (Fig. 10a) signalizes confined mobility of the chains, and the feature of anomalous diffusion behavior increases (lower values of d). In the gel-breakage regime, the movement of the chains becomes gradually less restricted and d approaches a value of 1 (Fickian diffusion), where the molecular displacements are not correlated. At this stage, the power-law attribute disappears and the long-time tail of the correlation function can be portrayed by a stretched exponential. Previous DLS studies on gelling systems of various natures have reported[20,21,26,27,29,50] values of d in the approximate range 0.1–0.5, and it is usually observed that the value of d decreases as the gel point is approached.

The parameter V is the time at which the power-law tail begins, and the time evolution of this quantity during the cross-linker process is illustrated in Figure 10b.

The general trend is that the value of V is shifted toward shorter times as the viscosity maximum is approached. In the gel-breakage regime, V exhibits a marked increase as the associations are disrupted. This finding suggests that when the local constraints are reduced, the onset of the power-law domain is shifted toward later times and the contribution of the fast relaxation mode becomes more pronounced. This indicates that the number and strength of cross-linking junctions in the network determine the start of the power-law regime. Our hypothesis is that the power-law feature of the correlation function is a signature of confined chain mobility in the system.

The angular dependence of the different parameters, obtained by fitting Eq 8a or 8b to the correlation functions at various stages during the cross-linker reaction is summarized in Figure 11. The fast mode (Fig. 11a) is always found to be diffusive ($\tau_f^{-1} \sim q^2$), and in the semidilute concentration regime the cooperative diffusion coefficient is probed, which reflects a concerted motion of polymer chains relative to the solvent.[39] The q dependence of the slow relaxation time ($\tau_s \sim q^{-2.5-3}$) is stronger (Fig. 11b) than that of a diffusive process. This behavior is characteristic of intraparticle dynamics and may arise from large-scale heterogeneities in the system. A stronger q dependence of the slow mode than that of the fast one has been reported from a number of DLS investigations on associating[51,52] polymer systems and gelling[22,27,53,54] samples. This feature is frequently ascribed to the formation of large clusters.

Let us now discuss the angular dependences of the parameters characterizing the power-law tails of the correlation functions. The q dependence of the inverse short-time cutoff of the power-law tail is roughly q^2 dependent ($V^{-1} \sim q^2$) although there is considerable fluctuation in the data (Fig. 11c). This q^2-dependence has been observed previously[20] for gelling systems, and this behavior indicates that in some sense diffusion dominates the dynamics. For incipient Pluronic gels, weaker q dependence ($V^{-1} \sim q^1$) was reported.[29] The q dependence of V^{-1} is probably related to the structure of the gel and the confinement of the chain dynamics. Figure 11d demonstrates the q dependence of the power-law tail exponent of the correlation functions. For the incipient gel, d appears to be q dependent ($d \sim q^1$), whereas in the gel-breakage regime d is almost independent of q. In view of this result, our conjecture is that the q dependence is a harbinger of hindered chain movement. Since the dimensional scale is altered with q, it is reasonable that the effect of displacement restrictions is changed. Actually, a q dependence of the power-law exponent b (see the discussion above) for incipient Pluronic gels has been reported from PFG NMR experiments.[49] It has been argued[27] that a q dependence of d implies the emergence of a new length scale. Previous DLS studies on gelling systems have reported different q dependences of d. For silica gels[20] a q independence was found, whereas a $d \sim q^1$ was reported for Pluronic gels,[29] and for gelatin gels[27] d was observed to exhibit a stronger q dependence ($d \sim q^2$).

4. Conclusions

In this work, we utilized rheological and dynamic light scattering methods to monitor the formation and destruction of gels formed from semidilute solutions of hyaluronic acid in the presence of different chemical cross-linker agents. It is demonstrated that the addition of water-soluble carbodiimide to the solution generates a gel after a certain time, and gradually the absolute value of the complex viscosity passes through a maximum but the ubiquitous competition between interpolymer cross-linking and hydrolysis of ester linkages and glycosidic bonds will steadily breakdown the network and a low-viscous solution is finally obtained. In this process, the large clusters are disintegrated, and the degradation of the polymer produces low-molecular weight species. If pH of the HA solution is changed, both the gelation characteristics and the rate of disruption of the gel are affected. At a low pH, the gelation time is long and it takes long time for the degradation of the gel. At a high pH, no gel is formed and there is a continuous breakdown of the solution in the course of a short period.

When L-lysineME is added to the HA solution containing WSC at a given pH, a longer gelation time is observed and the breakage of the gel is postponed, because of the formation of some amide linkages that are less sensitive to hydrolysis. By using the Ugi multicomponent condensation reaction, interpolymer cross-linking occurs via the formation of amide linkages and a stable gel evolves, which only exhibits a minor hydrolysis over a very long time. Even with a low cross-linker concentration, the gelation is fast and a strong gel is formed. At the gel point, the storage and loss moduli show a power-law behavior for all the systems, $G' \propto G'' \propto \omega^n$, with angular frequency ω.

The dynamic light scattering experiments reveal the emergence of a power-law tail in the correlation function at conditions in both the pregel and the postgel region. The decay at short times can be described by a stretched exponential, which yields the cooperative diffusion coefficient in the semidilute concentration regime. The power-law behavior is ascribed to anomalous diffusion, which is associated with gelling systems where confined chain dynamics prevails. Far beyond the viscosity maximum, the value of the power-law exponent d approaches 1 and uncorrelated chain movements in the system reign. The onset of the power-law regime is shifted toward longer times as the gel is weakened, and at a late stage in the gel-breaking regime the

power-law tail disappears and the profile of the long-time tail of the correlation function is portrayed by a stretched exponential. This slow mode exhibits an angular dependence (approximate q^3 dependence) that is stronger than that of a diffusive process. This is attributed to the formation of large clusters.

The inverse short-time cutoff of the power-law tail was found to be approximately q^2 dependent ($V^{-1} \sim q^2$), which seems to be a harbinger of diffusion-like dynamics. The power-law exponent d is q dependent ($d \sim q^1$) around the gel point and at a late stage in the gel-breaking regime d is approximately q independent. The q dependence is associated with restricted movement of the chains.

In this work, we have characterized some novel features in connection with the formation and destruction of chemical HA gels at different cross-linker conditions. We have demonstrated that the ester linkages formed in HA systems and glycosidic bonds are sensitive to hydrolysis, whereas the amide linkages formed via the Ugi multicomponent condensation reaction are very resistant against hydrolysis. We have also provided some evidence for that the power-law tail in the correlation function is associated with restricted chain dynamics. This is the first study where rheological and dynamical features during the chemical gelation and gel breakage of HA samples have been characterized.

Acknowledgements

A.M. and B.N. gratefully acknowledge financial support provided by a FUNMAT Project (Novel functional polymer materials for drug delivery applications). We thank Professor Lars Skattebøl, Dr. Trond Vidar Hansen, and Dr. Kaizheng Zhu for instructive comments concerning the various cross-linker reactions.

References

1. Yui, N.; Okano, T.; Sakurai, Y. *J. Controlled Release* **1992**, *22*, 105–116.
2. Pouyani, T.; Prestwich, G. D. *Bioconjugate Chem.* **1994**, *5*, 339–347.
3. Vercruysse, K. P.; Prestwich, G. D. *Crit. Rev. Ther. Drug Carrier Syst.* **1998**, *15*, 513–555.
4. Etienne, O.; Schneider, A.; Taddei, C.; Richert, L.; Schaaf, P.; Voegel, J.-C.; Egles, C.; Picart, C. *Biomacromolecules* **2005**, *6*, 726–733.
5. Kostko, A. F.; Chen, T.; Payne, G. F.; Anisimov, M. A. *Physica A* **2003**, *323*, 124–138.
6. Kuo, J. W.; Swann, D. A.; Prestwich, G. D. *Bioconjugate Chem.* **1991**, *2*, 232–241.
7. Tomihata, K.; Ikada, Y. *J. Biomed. Mater. Res.* **1997**, *37*, 243–251.
8. Nakajima, N.; Ikada, Y. *Bioconjugate Chem.* **1995**, *6*, 123–130.
9. Ugi, I.; Lohberger, S.; Karl, R. The Passerini and Ugi Reactions. In *Comprehensive Organic Synthesis*; Trost, B. M., Heathcock, C. H., Eds.; Pergamon: Oxford, UK, 1991; Vol. 2, pp 1083–1107.
10. de Nooy, A. E. J.; Masci, G.; Crescenzi, V. *Macromolecules* **1999**, *32*, 1318–1320.
11. de Nooy, A. E. J.; Capitani, D.; Masci, G.; Crescenzi, V. *Biomacromolecules* **2000**, *1*, 259–267.
12. Crescenzi, V.; Francescangeli, A.; Capitani, D.; Mannina, L.; Renier, D.; Bellini, D. *Carbohydr. Polym.* **2003**, *53*, 311–316.
13. Bu, H.; Kjøniksen, A.-L.; Knudsen, K. D.; Nyström, B. *Biomacromolecules* **2004**, *5*, 1470–1479.
14. Maleki, A.; Kjøniksen, A.-L.; Nyström, B. *Polym. Bull.* **2007**, *59*, 217–226.
15. Sannino, A.; Pappadà, S.; Madaghiele, M.; Maffezzoli, A.; Ambrosio, L.; Nicolais, L. *Polymer* **2005**, *46*, 11206–11212.
16. Scanlan, J. C.; Winter, H. H. *Macromolecules* **1991**, *24*, 47–54.
17. Winter, H. H. *Prog. Colloid Polym. Sci.* **1987**, *75*, 104–110.
18. Winter, H. H.; Chambon, F. *J. Rheol.* **1986**, *30*, 367–382.
19. Siegert, A. J. F. Massachusetts Institute of Technology Rad. Lab. Rep. No. 456, 1943.
20. Martin, J. E.; Wilcoxon, J.; Odinek, J. *Phys. Rev. A* **1991**, *43*, 858–872.
21. Lang, P.; Burchard, W. *Macromolecules* **1991**, *24*, 814–815.
22. Nyström, B.; Lindman, B. *Macromolecules* **1995**, *28*, 967–974.
23. Maleki, A.; Kjøniksen, A.-L.; Knudsen, K. D.; Nyström, B. *Polym. Int.* **2006**, *55*, 365–374.
24. Kohlrausch, R. *Pogg. Ann.* **1847**, *72*, 353–405.
25. Williams, G.; Watts, D. C. *Trans. Faraday Soc.* **1970**, *66*, 80–85.
26. Martin, J. E.; Adolf, D. *Annu. Rev. Phys. Chem.* **1991**, *42*, 311–339.
27. Ren, S. Z.; Shi, W. F.; Zhang, W. B.; Sorensen, C. M. *Phys. Rev. A* **1992**, *45*, 2416–2422.
28. Ren, S. Z.; Tombácz, E.; Rice, J. A. *Phys. Rev. E* **1996**, *53*, 2980–2983.
29. Nyström, B.; Kjøniksen, A.-L. *Langmuir* **1997**, *13*, 4520–4526.
30. Ikkai, F.; Shibayama, M. *Phys. Rev. Lett.* **1999**, *82*, 4946–4949.
31. Aoki, Y.; Norisuye, T.; Tran-Cong-Miyata, Q.; Nomura, S.; Nomura, S.; Sugimoto, T. *Macromolecules* **2003**, *36*, 9935–9942.
32. Ngai, K. L. *Adv. Colloid Interface Sci.* **1996**, *64*, 1–43.
33. Durand, D.; Delsanti, M.; Adam, M.; Luck, J. M. *Europhys. Lett.* **1987**, *3*, 297–301.
34. Adolf, D.; Martin, J. E.; Wilcoxon, J. P. *Macromolecules* **1990**, *23*, 527–531.
35. Koike, A.; Nemoto, N.; Takahashi, M.; Osaki, K. *Polymer* **1994**, *35*, 3005–3010.
36. Kjøniksen, A.-L.; Nyström, B. *Macromolecules* **1996**, *29*, 5215–5222.
37. Clark, A. H.; Ross-Murphy, S. B. *Adv. Polym. Sci.* **1987**, *83*, 57–192.
38. Nyström, B.; Walderhaug, H.; Hansen, F. K.; Lindman, B. *Langmuir* **1995**, *11*, 750–757.
39. De Gennes, P. G. *Scaling Concepts in Polymer Physics*; Cornell University Press: Ithaca, NY, 1979.
40. Martin, J. E.; Adolf, D.; Wilcoxon, J. P. *Phys. Rev. Lett.* **1988**, *61*, 2620–2623; . *Phys. Rev. A* **1989**, *39*, 1325–1332.
41. Rubinstein, M.; Colby, R. H. *Macromolecules* **1994**, *27*, 3184–3190.

42. Okamoto, M.; Norisuye, T.; Shibayama, M. *Macromolecules* **2001**, *34*, 8496–8502.
43. Shukla, A.; Fuchs, R.; Rehage, H. *Langmuir* **2006**, *22*, 3000–3006.
44. Doi, M.; Onuki, A. *J. Phys. II France* **1992**, *2*, 1631–1656.
45. Hecht, A.-M.; Guillermo, A.; Horkay, F.; Mallam, S.; Legrand, J. F.; Geissler, E. *Macromolecules* **1992**, *25*, 3677–3684.
46. Gefen, Y.; Aharony, A.; Alexander, S. *Phys. Rev. Lett.* **1983**, *50*, 77–80.
47. Sahimi, M.; Hughes, B. D.; Scriven, L. E.; Davis, H. T. *J. Chem. Phys.* **1983**, *78*, 6849–6864.
48. Widom, A.; Chen, H. J. *J. Phys. A: Math. Gen.* **1995**, *28*, 1243–1247.
49. Walderhaug, H.; Nyström, B. *J. Phys. Chem. B* **1997**, *101*, 1524–1528.
50. Konák, C.; Bansil, R. *Il Nuovo Cimento* **1994**, *16D*, 689–696.
51. Nyström, B.; Thuresson, K.; Lindman, B. *Langmuir* **1995**, *11*, 1994–2002.
52. Thuresson, K.; Nilsson, S.; Kjøniksen, A.-L.; Walderhaug, H.; Lindman, B.; Nyström, B. *J. Phys. Chem. B* **1999**, *103*, 1425–1436.
53. Martin, J. E.; Wilcoxon, J. P. *Phys. Rev. Lett.* **1988**, *61*, 373–376.
54. Adam, M.; Delsanti, M.; Munch, J. P.; Durand, D. *Phys. Rev. Lett.* **1988**, *61*, 706–709.